

UNCLASSIFIED

AD 400 708

*Reproduced
by the*

**ARMED SERVICES TECHNICAL INFORMATION AGENCY
ARLINGTON HALL STATION
ARLINGTON 12, VIRGINIA**



UNCLASSIFIED

NOTICE: When government or other drawings, specifications or other data are used for any purpose other than in connection with a definitely related government procurement operation, the U. S. Government thereby incurs no responsibility, nor any obligation whatsoever; and the fact that the Government may have formulated, furnished, or in any way supplied the said drawings, specifications, or other data is not to be regarded by implication or otherwise as in any manner licensing the holder or any other person or corporation, or conveying any rights or permission to manufacture, use or sell any patented invention that may in any way be related thereto.

63-3-1

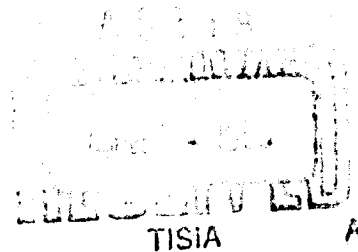
NOLTR 62-111

400708

LOGGED BY ASTIA

AD NO.

APPROXIMATE ANALYSIS OF EFFECT ON
DRAG OF TRUNCATING THE CONICAL NOSE
OF A BODY OF REVOLUTION IN SUPERSONIC
FLOW



NOL

1 DECEMBER 1962

UNITED STATES NAVAL ORDNANCE LABORATORY, WHITE OAK, MARYLAND

NOLTR 62-111

- RELEASED TO ASTIA
BY THE NAVAL ORDNANCE LABORATORY
- ☒ Without restrictions
 - ☐ For Release to Military and Government Agencies Only.
 - ☐ Approval by BuWeps required for release to contractors.
 - ☐ Approval by BuWeps required for all subsequent release.

Aerodynamics Research Report No. 183

APPROXIMATE ANALYSIS OF EFFECT ON DRAG OF TRUNCATING
THE CONICAL NOSE OF A BODY OF REVOLUTION IN
SUPERSONIC FLOW

by
Neal Tetervin

ABSTRACT: A rapid method for estimating the nose pressure-drag coefficient in supersonic flow of a body formed by replacing all, or part of, its conical nose by a flat face is derived. The analysis, although rough, agrees with the experimental observation that the drag coefficient of a flat-faced cone of fixed length decreases as the radius of the flat face increases from zero. After reaching a minimum, the drag coefficient rises above that of the sharp-tipped cone.

PUBLISHED FEBRUARY 1963

U. S. NAVAL ORDNANCE LABORATORY
WHITE OAK, MARYLAND

NOLTR 62-111

1 December 1962

**Approximate Analysis of Effect on Drag of Truncating the
Conical Nose of a Body of Revolution in Supersonic Flow**

This report presents a rapid method for estimating the nose pressure-drag coefficient in supersonic flow of a body formed by replacing all, or part of, its conical nose by a flat face.

It is noted that, if the nose length is not decreased, a sharp nose can be replaced by a flat nose of appreciable area without increasing the drag above that for the sharp nose.

This work was sponsored by the Re-Entry Body Section of the Special Projects Office, Bureau of Naval Weapons under the Applied Research Program in Aeroballistics, Task No. NOL-363.

R. E. ODENING
Captain, USN
Commander

K. R. Enkenhus
K. R. ENKENHUS
By direction

CONTENTS

	Page
SUMMARY	1
INTRODUCTION	2
ANALYSIS	2
Change in Nose Pressure-Drag When Part of Conical Tip is Cut Off to Form Flat Face	2
Change in Nose Pressure-Drag When Conical Tip is Replaced by Flat Face but Nose Length is Fixed	6
Comparison with Experiment	12
CONCLUDING REMARKS	14
REFERENCES	15

SYMBOLS

A	defined in equation (30)
B	defined in equation (31)
C_D	nose drag coefficient $\frac{\bar{D}}{(\frac{\rho}{2} V^2)_{\infty} \pi R^2}$
$\Delta C_{Dn,m}$	drag coefficient of body (n) minus drag coefficient of body (m)
\bar{D}	nose pressure drag
$\Delta \bar{D}_{2,1}$	pressure drag of body (2) minus pressure drag of body (1)
\bar{Y}_1	length of portion of body (1) that is to be replaced, measured along surface from most forward point (see fig. 1(b))
\bar{Y}_2	length of portion of body (2) that is different from body (1), measured from most forward point (see fig. 1(b))
F	quantity, $\frac{2}{\gamma M^2} \frac{\bar{p}_0}{\bar{p}_\infty} \left[2 \int_0^1 \frac{\bar{M}}{\bar{p}_0} \frac{\bar{X}}{H} d\frac{\bar{X}}{H} - \left(\frac{\bar{p}_e}{\bar{p}_0} \right)_c \right]$
H	radius of flat face
I	non-dimensional pressure integral over flat face, $\int_0^1 \frac{\bar{p}_e}{\bar{p}_0} \frac{\bar{X}}{H} d\frac{\bar{X}}{H}$
L	distance from most forward to most rearward point of axis of symmetry, measured along surface (see fig. 1(a))
M	Mach number
\bar{N}	length of nose measured along axis of body
\bar{p}	static pressure
$\frac{\Delta \bar{p}}{q}$	non-dimensional pressure coefficient $\frac{\bar{p}_e - \bar{p}_\infty}{\left(\frac{\rho}{2} V^2 \right)_{\infty}}$

SYMBOLS

\bar{q}	dynamic pressure $\left(\frac{\rho v^2}{2}\right)_\infty$
\bar{r}	radius of cross-section of body, perpendicular to axis of symmetry (see fig. 1(a))
R	radius of reference cross-section of body
V	velocity of flight
X	distance along surface of body from most forward point on axis of symmetry (see fig. 1(a))
γ	ratio of specific heats
ϵ	tangent of cone half angle
Θ	angle between tangent to body surface and axis of symmetry (see fig. 1(a))
$\bar{\rho}$	density

Subscripts

o	at stagnation point behind a normal shock
e	local value on body
∞	in free stream ahead of bow shock
C	value on cone
$(n), \text{ or } n$	pertaining to body number n
N	for fixed nose length
Θ	for fixed cone angle
S	with sharp tip
—	quantities with a bar are dimensional, unbarred quantities are non-dimensional
	all non-dimensional lengths are based on the reference length R
B	value for which C_D of flat-face cone equals C_D of sharp cone

SUMMARY

A rapid method for estimation of the nose pressure-drag coefficient in supersonic flow of a body formed by replacing all, or part of, its conical nose by a flat face is given. The analysis, although rough, agrees with the experimental observation that the drag coefficient of a truncated cone of fixed length decreases as the radius of the flat face increases from zero. After reaching a minimum, the drag coefficient rises above that of the sharp-tipped cone. For example, at a Mach number of 2.4, the calculated nose drag coefficient of a truncated cone, obtained from a sharp-tipped cone of 38° included angle by decreasing the cone angle without changing the nose length, decreases to about 93 percent of that of the sharp cone as the flat-face radius increases to 15 percent of the base radius. The drag coefficient of the blunt cone remains less than that for the sharp cone up to a ratio of flat face to base radius of about 28 percent.

At a Mach number of 2.4, the calculated nose drag coefficient of a flat-faced cone, obtained from a sharp cone of 38° included angle by decreasing the cone angle, is as much as 19 percent less than the nose drag of the cone of equal flat-face area obtained by keeping the cone angle fixed at 38° and reducing the nose length.

The indication from the analysis is that the allowable blunting for no increase in drag over the sharp cone decreases slowly with increase in Mach number and more rapidly with decrease in sharp cone angle.

The method for the estimation of the change in drag coefficient caused by keeping the cone angle fixed and cutting off part of the nose to form a flat face is tested by comparison with experimental results in two cases. In the first, the method predicts the drag coefficient of a flat-faced cylinder from that of a sharp-nose cone with a maximum error of about 5 percent. In the second, the method predicts the drag coefficient of a flat-faced cone-cylinder from that for a sharp-nose cone-cylinder with a maximum error of about 16 percent.

INTRODUCTION

It is sometimes necessary to estimate the change in drag coefficient caused by cutting off the forward portion of a flat-faced body in supersonic flow. In the present investigation, the portion of the body that is cut off to form a new and larger flat face is the frustrum of a cone. Because the method of analysis of the change in drag is rough, a search of the literature was made in order to obtain experimental data for a test of the method of analysis. References (1) and (2) were found to contain data that were useful for testing the method of analysis. A statement in reference (2), that an extrapolation of the experimental results predicted that the drag of a flat-faced cone of fixed nose length would be less than that for the sharp cone, was noted.

The search of the literature also disclosed that some time ago reference (3) had reached the result that cones tipped by spheres could have less drag than sharp cones. Reference (3) gives experimental and theoretical curves of drag coefficient that demonstrate this effect. Although a short description of the method by which the drag coefficient was calculated is given, no equations are given. Moreover, it is not clear whether or not the result that the drag decreases as the sharp tip is blunted was obtained from an examination of the results of calculations or from an examination of equations. In the present investigation, equations are given, and it is apparent from them that the drag coefficient of a cone initially decreases when the tip is blunted and the nose length is kept fixed. Moreover, the present rough analysis indicates that the flat face can be made fairly large in diameter before the drag of the blunt cone exceeds that of the sharp cone.

The present investigation treats only a special case of the supersonic drag problem. It does not attempt to discuss the problem of minimum drag bodies, a subject that has already been fully treated by many investigators by more exact methods of analysis.

ANALYSIS

Change in Nose Pressure-Drag When Part of Conical Tip is Cut Off to Form Flat Face

The drag is assumed to consist of pressure drag only; the friction drag is neglected. The pressure drag is

$$\bar{D} = \int_0^L \bar{p}_e \sin \theta \, 2\pi \bar{r} \, d\bar{x} \quad (1) \text{ (see fig. 1(a))}$$

For the body denoted by (1) in figure 1(b), the drag is

$$\overline{D}_1 = \int_0^{\overline{L}_1} \overline{p}_e \sin \theta 2\pi \overline{r} d\overline{x} = \int_0^{\overline{f}_1} \overline{p}_e \sin \theta 2\pi \overline{r} d\overline{x} + \int_{\overline{f}_1}^{\overline{L}_1} \overline{p}_e \sin \theta 2\pi \overline{r} d\overline{x} \quad (2)$$

For the body denoted by (2), the drag is

$$\overline{D}_2 = \int_0^{\overline{L}_2} \overline{p}_e \sin \theta 2\pi \overline{r} d\overline{x} = \int_0^{\overline{f}_2} \overline{p}_e \sin \theta 2\pi \overline{r} d\overline{x} + \int_{\overline{f}_2}^{\overline{L}_2} \overline{p}_e \sin \theta 2\pi \overline{r} d\overline{x} \quad (3)$$

Because the forward portion of body (1) is cut off to form body (2), the interval length $(\overline{L}_1 - \overline{f}_1)$ is equal to the length $(\overline{L}_2 - \overline{f}_2)$ and \overline{r} and θ are the same functions of $(\overline{x} - \overline{f}_1)$ as of $(\overline{x} - \overline{f}_2)$. It is also assumed that \overline{p}_e is the same function of $(\overline{x} - \overline{f}_1)$ as of $(\overline{x} - \overline{f}_2)$, that is, that the static pressure on the remaining portion of the body is unchanged by removing its forward portion. Consequently,

$$\int_{\overline{f}_1}^{\overline{L}_1} \overline{p}_e \sin \theta 2\pi \overline{r} d\overline{x} = \int_{\overline{f}_2}^{\overline{L}_2} \overline{p}_e \sin \theta 2\pi \overline{r} d\overline{x} \quad (4)$$

Therefore,

$$\Delta \overline{D}_{2,1} = \overline{D}_2 - \overline{D}_1 = \int_0^{\overline{f}_2} \overline{p}_e \sin \theta 2\pi \overline{r} d\overline{x} - \int_0^{\overline{f}_1} \overline{p}_e \sin \theta 2\pi \overline{r} d\overline{x} \quad (5)$$

or

$$\Delta C_{D,1} = \frac{\Delta \overline{D}_{2,1}}{\left(\frac{\overline{p}_0}{2}\right) \pi \overline{R}^2} = \frac{2 \overline{p}_0}{\left(\frac{\overline{p}_0}{2}\right)} \int_0^{\overline{f}_2} \frac{\overline{p}_e}{\overline{p}_0} \frac{\overline{r}}{\overline{R}} \sin \theta d\frac{\overline{x}}{\overline{R}} - \frac{2 \overline{p}_0}{\left(\frac{\overline{p}_0}{2}\right)} \int_0^{\overline{f}_1} \frac{\overline{p}_e}{\overline{p}_0} \frac{\overline{r}}{\overline{R}} \sin \theta d\frac{\overline{x}}{\overline{R}} \quad (6)$$

but

$$\frac{\overline{p}_0}{\left(\frac{\overline{p}_0}{2}\right)} = \frac{\overline{p}_0}{\overline{p}_\infty} \frac{2}{\gamma M^2}$$

then

$$\Delta C_{D,1} = \frac{4 \left(\frac{\overline{p}_0}{\overline{p}_\infty}\right)}{\gamma M^2} \left[\int_0^{\overline{f}_2} \frac{\overline{p}_e}{\overline{p}_0} (\sin \theta) \overline{r} d\overline{x} - \int_0^{\overline{f}_1} \frac{\overline{p}_e}{\overline{p}_0} (\sin \theta) \overline{r} d\overline{x} \right] \quad (7)$$

Equation (7) applies for any body of revolution that is modified by changing its forward portion in an arbitrary manner, provided that the assumption that \bar{p}_e is the same function of $(\bar{x} - \bar{f}_1)$ as of $(\bar{x} - \bar{f}_2)$ is valid. Actually, however, \bar{p}_e for $\bar{x} > \bar{f}_2$ is different from \bar{p}_e for $\bar{x} > \bar{f}_1$. The difference is largest at $\bar{x} = \bar{f}_2$ and decays downstream.

When the modified body, body (2), has a flat face, the conditions $\sin\theta = 1$, $\bar{r} = \bar{x}$ apply for $0 \leq \bar{x} \leq \bar{f}_2$, the flat face region. When the body (1) is conical over the "cut-off" portion, the conditions $\sin\theta = \text{const.}$, $\bar{r} = \bar{x}\sin\theta$ apply for $0 \leq \bar{x} \leq \bar{f}_1$. In this case, equation (7) becomes

$$\Delta C_{D_{2,1}} = \frac{4\left(\frac{\bar{p}_e}{\bar{p}_0}\right)}{\gamma M^2} \left[\int_0^{\bar{f}_2} \frac{\bar{p}_e}{\bar{p}_0} \bar{x} d\bar{x} - \sin^2\theta \int_0^{\bar{f}_1} \frac{\bar{p}_e}{\bar{p}_0} \bar{x} d\bar{x} \right] \quad (8)$$

It is more convenient to non-dimensionalize the length \bar{x} in the first integral of equation (8) by the radius of the flat face H , than by the reference radius R . Thus,

$$\int_0^{\bar{f}_2} \frac{\bar{p}_e}{\bar{p}_0} \bar{x} d\bar{x} = \int_0^{\bar{f}_2} \frac{\bar{p}_e}{\bar{p}_0} \frac{\bar{x}}{R} d\frac{\bar{x}}{R} = \left(\frac{H_2}{R}\right)^2 \int_0^1 \frac{\bar{p}_e}{\bar{p}_0} \frac{\bar{x}}{H_2} d\frac{\bar{x}}{H_2}$$

or

$$\int_0^{\bar{f}_2} \frac{\bar{p}_e}{\bar{p}_0} \bar{x} d\bar{x} = H_2^2 \int_0^1 \frac{\bar{p}_e}{\bar{p}_0} \frac{\bar{x}}{H_2} d\frac{\bar{x}}{H_2} \quad (9)$$

Because the body is conical for x less than f_1 , $\frac{\bar{p}_e}{\bar{p}_0}$ is constant and equal to the value for a cone. Consequently,

$$\int_0^{\bar{f}_1} \frac{\bar{p}_e}{\bar{p}_0} \bar{x} d\bar{x} = \left(\frac{\bar{p}_e}{\bar{p}_0}\right)_c \frac{\bar{f}_1^2}{2}$$

but

$$\bar{f}_1 \sin\theta = H_2$$

therefore,

$$\sin^2\theta \int_0^{\bar{f}_1} \frac{\bar{p}_e}{\bar{p}_0} \bar{x} d\bar{x} = \left(\frac{\bar{p}_e}{\bar{p}_0}\right)_c \frac{H_2^2}{2} \quad (10)$$

When the relations (9) and (10) are used, equation (8) becomes

$$\Delta C_{D_{2,1}} = \frac{2\left(\frac{\bar{p}_e}{\bar{p}_0}\right)}{\gamma M^2} H_2^2 \left[2 \int_0^1 \frac{\bar{p}_e}{\bar{p}_0} \frac{\bar{x}}{H_2} d\frac{\bar{x}}{H_2} - \left(\frac{\bar{p}_e}{\bar{p}_0}\right)_c \right] \quad (11)$$

To find the change in drag between two different "cut-offs" for the same body when the section removed is conical, use is made of equation (11). Both "cut-off" bodies, referred to as bodies (3) and (4), have flat faces. The change in drag is

$$\Delta \bar{D}_{4,3} = \bar{D}_4 - \bar{D}_3$$

or

$$\Delta \bar{D}_{4,3} = (\bar{D}_1 + \Delta \bar{D}_{4,1}) - (\bar{D}_1 + \Delta \bar{D}_{3,1}) \quad (12)$$

where $\Delta \bar{D}_{4,1}$ and $\Delta \bar{D}_{3,1}$ are the differences between the drag of bodies (4) and (3) respectively and the body with a conical tip. Equation (12) can be written as

$$\Delta \bar{D}_{4,3} = \Delta \bar{D}_{4,1} - \Delta \bar{D}_{3,1}$$

or

$$\Delta C_{D_{4,3}} = \Delta C_{D_{4,1}} - \Delta C_{D_{3,1}} \quad (13)$$

The reference radius \bar{R} remains fixed although the nose shape is changed.

By assuming that the integral $\int_0^{\bar{p}_e} \frac{\bar{x}}{\bar{H}} d\bar{x}$ is the same over the flat faces of bodies (3) and (4) and by combining equation (13) with equation (11), in which the subscript "2" is replaced first by "4" and then by "3", the result is obtained that

$$\Delta C_{D_{4,3}} = \frac{2}{\gamma M^2} \left(\frac{\bar{p}_\infty}{\bar{p}_e} \right) \left[2\mathcal{I} - \left(\frac{\bar{p}_e}{\bar{p}_\infty} \right) \right] (H_4^2 - H_3^2) \quad (14)$$

where

$$\mathcal{I} = \int_0^{\bar{p}_e} \frac{\bar{p}_e}{\bar{p}_\infty} \frac{\bar{x}}{\bar{H}} d\bar{x}$$

The quantity

$$\frac{2}{\gamma M^2} \left(\frac{\bar{p}_\infty}{\bar{p}_e} \right) \left[2\mathcal{I} - \left(\frac{\bar{p}_e}{\bar{p}_\infty} \right) \right]$$

depends on the Mach number and on the angle of the conical nose. Call this quantity F ; equation (14) then becomes

$$\Delta C_{D_{4,3}} = (H_4^2 - H_3^2) F \quad (15)$$

and equation (11) becomes

$$\Delta C_{D_{2,1}} = H_2^2 F \quad (16)$$

EXAMPLE: A numerical value of the integral $\int_0^1 \frac{\bar{p}_e}{\bar{p}_0} \frac{\bar{x}}{H} d\frac{\bar{x}}{H}$ in the function F is obtained by using the distribution of \bar{p}_e over the flat face of a cylinder at a Mach number near 2 presented in figure 7 of reference (4). The integral then has the value .453. The pressure distribution of reference (4), and thus the value .453 for the integral, is assumed to be independent of Mach number. The cone pressure ratio $\left(\frac{\bar{p}_e}{\bar{p}_0}\right)_c$ is calculated from the identity

$$\left(\frac{\bar{p}_e}{\bar{p}_0}\right)_c = \frac{\bar{p}_\infty}{\bar{p}_0} \left(1 + \frac{\gamma M^2}{2} \frac{\Delta \bar{p}}{\bar{q}}\right) \quad (17)$$

where the quantities $\frac{\Delta \bar{p}}{\bar{q}}$ and $\frac{\bar{p}_\infty}{\bar{p}_0}$ are read from the charts and tables of reference (5). The quantity F is shown in figure 2 for the Mach number range between 3 and 1.19 for a body whose nose is a cone of 38° included angle. The lowest Mach number, namely, 1.19, is that at which the bow shock detaches from the conical nose. According to figure 2, F is equal to 1.250 at a Mach number of 2.4. Then, if H_4 is equal to .3 and H_3 is equal to .2, the value of $\Delta C_{D_{4,3}}$ is .0625.

Change in Nose Pressure-Drag When Sharp Tip is Replaced by Flat Face but Nose Length is Fixed

In reference (2) it is noted that an extrapolation of the experimental data predicts that the drag of a cone can be decreased by substituting a blunt tip for the sharp tip while keeping the nose length fixed. This effect is also noted in reference (3), and a calculated variation of drag coefficient with the ratio of nose radius to maximum radius is given for a cone capped by a spherical tip. No equations for making the calculations are given, however, but it is stated that the pressure on the conical portion of the blunt cone was assumed to be equal to that of a sharp cone of the same angle. The pressure on the hemispherical nose was obtained from experiment.

As a matter of interest, an investigation was made to ascertain whether or not the present procedure would predict a decrease in cone drag if the sharp tip is replaced by a flat

portion without a change in nose length. The pressure drag of a flat-faced cone is found by adding the nose drag coefficient of the sharp cone

$$C_D = \frac{2}{\gamma M^2} \left(\frac{\bar{p}_o}{\bar{p}_\infty} \right) \left(\frac{\bar{p}_e}{\bar{p}_o} \right)_c \quad (18)$$

to $\Delta C_{D2,1}$ given by equation (11). The result is

$$C_D = \frac{4}{\gamma M^2} \left(\frac{\bar{p}_o}{\bar{p}_\infty} \right) \left[H^2 I + \left(\frac{\bar{p}_e}{\bar{p}_o} \right)_c \frac{1-H^2}{2} \right] \quad (19)$$

When the cone tip is replaced by a flat face without changing the cone angle, the ratio $\left(\frac{\bar{p}_e}{\bar{p}_o} \right)_c$ is called $\left(\frac{\bar{p}_e}{\bar{p}_o} \right)_{c,\theta}$ and the drag coefficient is called $C_{D\theta}$. When the nose length is unchanged, the cone angle is decreased by substitution of a flat face for the sharp tip. In this case, the ratio $\left(\frac{\bar{p}_e}{\bar{p}_o} \right)_c$ is called $\left(\frac{\bar{p}_e}{\bar{p}_o} \right)_{c,N}$ and the drag coefficient is denoted by C_{DN} .

Equation (19) was used to calculate $C_{D\theta}$ and C_{DN} at a Mach number of 2.4 for a body that was originally a sharp-tipped cone of 38° included angle. The results are shown in figure 3. Also shown is the ratio $\frac{C_{D\theta} - C_{DN}}{C_{D\theta}}$. At a value

of H of about .34, this ratio has its maximum value, namely about .19. Consequently, at a Mach number of 2.4, the nose drag of the frustrum of a cone of 38° included angle and nose radius equal to .34 of the base radius is 19 percent larger than the nose drag of the frustrum of the cone with the same ratio of nose to base radius, but with the same nose length as the original sharp-tipped cone. The longer cone has an included angle of about 26° instead of 38° .

The value of H at which C_D is a minimum is obtained by differentiating equation (19) with respect to H and setting the derivative equal to zero. The derivative of C_D with respect to H is:

$$\frac{dC_D}{dH} = \frac{4}{\gamma M^2} \left(\frac{\bar{p}_o}{\bar{p}_\infty} \right) \left[2HI - \left(\frac{\bar{p}_e}{\bar{p}_o} \right)_c H + \frac{1-H^2}{2} \frac{d \left(\frac{\bar{p}_e}{\bar{p}_o} \right)_c}{dH} \right] \quad (20)$$

or with

$$\frac{d \left(\frac{\bar{p}_e}{\bar{p}_o} \right)_c}{dH} = \frac{d \left(\frac{\bar{p}_e}{\bar{p}_o} \right)_c}{d\theta} \frac{d\theta}{dH}$$

and with

$$\tan \theta = \frac{1-H}{N}$$

it follows that

$$\frac{dC_D}{dH} = \frac{4}{\gamma M^2} \left(\frac{\bar{p}_0}{\bar{p}_\infty} \right) \left[2HI - \left(\frac{\bar{p}_e}{\bar{p}_\infty} \right)_c H - \frac{1}{2} \frac{N(1-H^2)}{N^2 + (1-H)^2} \frac{d\left(\frac{\bar{p}_e}{\bar{p}_\infty}\right)_c}{d\theta} \right] \quad (21)$$

It is noted that because $\frac{d\left(\frac{\bar{p}_e}{\bar{p}_\infty}\right)_c}{d\theta}$ is positive, it follows that $\frac{dC_D}{dH} < 0$ for $H = 0$. That is, the nose-pressure drag coefficient of a cone always decreases with initial blunting. For a minimum C_D , it follows from setting $\frac{dC_D}{dH}$ equal to zero and from equation (21) that

$$\frac{H}{1-H^2} \left[(1-H)^2 + N^2 \right] = \frac{\frac{N}{2} \frac{d\left(\frac{\bar{p}_e}{\bar{p}_\infty}\right)_c}{d\theta}}{\left[2I - \left(\frac{\bar{p}_e}{\bar{p}_\infty}\right)_c \right]} \quad (22)$$

A calculation for

$$\begin{aligned} M &= 2.4 \\ I &= .453 \\ \text{and } N &= \frac{1}{\tan 19^\circ} = 2.904 \end{aligned}$$

predicts a minimum value of C_D at $H = .15$. The value of C_D is calculated to be .492.

In order to find the non-zero value of H , called H_B , at which the drag coefficient of the flat-faced cone is equal to the drag of a sharp cone of equal nose length, the drag coefficient given by equation (18) is equated to that given by equation (19). The result, after use of equation (17), is

$$H^2 = \frac{\left(\frac{\Delta \bar{p}}{\bar{q}}\right)_{c,s} - \left(\frac{\Delta \bar{p}}{\bar{q}}\right)_c}{\frac{2}{\gamma M^2} \left[2I \frac{\bar{p}_0}{\bar{p}_\infty} - 1 \right] - \left(\frac{\Delta \bar{p}}{\bar{q}}\right)_c} \quad (23)$$

where the first and second terms in the numerator refer to the sharp and blunt cone, respectively. The non-dimensional pressure difference $\left(\frac{\Delta \bar{p}}{\bar{q}}\right)_c$ for the blunt cone depends on θ and, therefore, on H . Equation (23) can be solved graphically or by some other convenient method. In the present example, a cone of half angle 19° , at $M = 2.4$, the value of H_B is about

.285. That is, the drag of the flat-faced cone is less than that of the sharp cone for H less than .285. For a cone of 10° half angle, the value of H_B drops to about .103. In figure 4 is shown the variation of H_B with sharp-cone angle at Mach numbers of 2.4 and 4.

The values of H_B for θ_s equal to 10° and to 19° were calculated by use of equation (23) together with Chart 6 and Table II of reference (5) for $\frac{\Delta \bar{p}}{q}$ and $\frac{p}{p_\infty}$ respectively.

The circles and squares in figure 4 are calculated values; the curves were drawn through these points. For sharp-cone angles of 5° and less, a sufficiently accurate value of H_B could not be obtained by use of Chart 6 of reference (5) because it was impossible to read the chart to enough significant figures. The values of $\frac{\Delta \bar{p}}{q}$ for $\theta_s = 5^\circ$ for $M = 2.4$ and 4, therefore,

were calculated by use of equation (7-36) of reference (6). The equation is

$$\begin{aligned} \frac{\Delta \bar{p}}{q} = & -\epsilon^2 + 2\epsilon^2 \ln \frac{2}{\epsilon \sqrt{M^2-1}} + 3(M^2-1)\epsilon^4 \left[\ln \frac{2}{\epsilon \sqrt{M^2-1}} \right]^2 \\ & - (5M^2-1)\epsilon^4 \ln \frac{2}{\epsilon \sqrt{M^2-1}} + \left[\frac{13}{4}M^2 + \frac{1}{2} + \frac{(r+1)M^4}{M^2-1} \right] \epsilon^4 \end{aligned} \quad (24)$$

According to reference (6), the value of $\frac{\Delta \bar{p}}{q}$ given by equation

(24) for a cone of 5° half angle cannot be distinguished from the exact values in figure E7d of reference 6; this figure compares exact values of $\frac{\Delta \bar{p}}{q}$ with values calculated by

approximate methods. The accuracy of equation (24) increases as the cone angle decreases below 5° .

For angles less than 5° , the value of H_B was calculated directly from an explicit expression for H_B . This expression was obtained by using $\epsilon = \frac{1}{N}$

for the sharp cone, and $\epsilon = \frac{1-H}{N}$

for the flat-faced cone. The result for $\left(\frac{\Delta \bar{p}}{q}\right)_{c,s}$ is, from equation (24),

$$\begin{aligned} \left(\frac{\Delta \bar{p}}{q}\right)_{c,s} = & -\frac{1}{N^2} + \frac{2}{N^2} \ln \frac{2N}{\sqrt{M^2-1}} + \frac{3(M^2-1)}{N^4} \left[\ln \frac{2N}{\sqrt{M^2-1}} \right]^2 \\ & - \frac{(5M^2-1)}{N^4} \ln \frac{2N}{\sqrt{M^2-1}} + \left[\frac{13}{4}M^2 + \frac{1}{2} + \frac{(r+1)M^4}{M^2-1} \right] \frac{1}{N^4} \end{aligned} \quad (25)$$

and for $\left(\frac{\Delta \bar{p}}{\bar{q}}\right)_c$ is,

$$\left(\frac{\Delta \bar{p}}{\bar{q}}\right)_c = -\frac{(1-H)^2}{N^2} + \frac{2(1-H)^2}{N^2} \ln \frac{2N}{(1-H)\sqrt{M^2-1}} + \frac{3(M^2-1)(1-H)^4}{N^4} \left[\ln \frac{2N}{(1-H)\sqrt{M^2-1}} \right]^2$$

$$- \frac{(5M^2-1)(1-H)^4}{N^4} \ln \frac{2N}{(1-H)\sqrt{M^2-1}} + \left[\frac{13}{4}M^2 + \frac{1}{2} + \frac{(7+1)M^4}{M^2-1} \right] \frac{(1-H)^4}{N^4}$$

In order to get an explicit expression for H_B , expression (26) is restricted to small values of H . For small values of H , the approximation that

$$\ln \frac{2N}{(1-H)\sqrt{M^2-1}} = \ln \frac{2N}{\sqrt{M^2-1}} + H + \frac{H^2}{2} \quad (27)$$

and that

$$(1-H)^2 \left(H + \frac{H^2}{2} \right) = H - \frac{3}{2} H^2 \quad (28)$$

is made. When expressions (25) and (26) are used in equation (23) together with the approximations (27) and (28), and all terms multiplied by H^3 or higher powers of H are neglected, the result, after collecting terms, is

$$H_B = \frac{A}{B} \quad (29)$$

where

$$A = 4N^2 \left(\ln \frac{2N}{\sqrt{M^2-1}} - 1 \right) - (26M^2 - 10) \ln \frac{2N}{\sqrt{M^2-1}}$$

$$+ 12(M^2-1) \left(\ln \frac{2N}{\sqrt{M^2-1}} \right)^2 + 18M^2 + 1 + 4 \frac{(7+1)M^4}{M^2-1} \quad (30)$$

and

$$B = \frac{2N^4}{8M^2} \left[2I \frac{\bar{p}_0}{\bar{p}_\infty} - 1 \right] - 3N^2 + 15(M^2-1) \left(\ln \frac{2N}{\sqrt{M^2-1}} \right)^2$$

$$- (46M^2 - 26) \ln \frac{2N}{\sqrt{M^2-1}} + \frac{17}{4}M^2 - 9 - 5 \frac{(7+1)M^4}{M^2-1} \quad (31)$$

The curves of figure 4 for $M = 2.4$ and 4 for $\theta_s < 5^\circ$ were calculated by use of equation (29). For $\theta_s = 5^\circ$, the value of H_B calculated by use of equation (29) differs from the value of H_B obtained by use of equations (23), (25) and (26) by less than 3 percent. Calculations indicate that expression (29)

rapidly becomes inaccurate for θ_s greater than about $7\frac{1}{2}^\circ$.

For half cone angles less than 2° or so, the value of N becomes large enough for equation (29) to be approximated with an error of no more than about 5 percent by,

$$H_B = \frac{4 \left(\ln \frac{2N}{M^2} - 1 \right)}{\frac{2N^2}{\gamma M^2} \left[2I \frac{\bar{p}_0}{\bar{p}_\infty} - 1 \right] - 3} \quad (32)$$

The indication from equation (32) is that for small cone angles, H_B increases somewhat more slowly than θ_s^2 .

Because H_B decreases with increase in M , (see fig. 4), it was of interest to determine how much further H_B would decrease from the values for $M = 4$ as M increased. A calculation of the variation of H_B with θ_s was, therefore, made for $M = \infty$. To calculate the value of H_B at $\theta_s = 10^\circ$ and at 19° , the Chart 6 of reference (5) was used to get $\left(\frac{\Delta \bar{p}}{\bar{p}} \right)_c$ for $M = \infty$. The value of the term

$$\frac{2}{\gamma M^2} \left[2I \frac{\bar{p}_0}{\bar{p}_\infty} - 1 \right]$$

for $M = \infty$ was calculated by keeping I equal to .453 and letting M become very large in the expression for $\frac{\bar{p}_0}{\bar{p}_\infty}$, namely,

$$\frac{\bar{p}_0}{\bar{p}_\infty} = \left(\frac{\gamma+1}{2} M^2 \right)^{\frac{\gamma}{\gamma-1}} \left[\frac{\gamma+1}{2\gamma M^2 - (\gamma-1)} \right]^{\frac{1}{\gamma-1}}$$

(ref. (5))

The result is

$$\frac{2}{\gamma M^2} \left[2I \frac{\bar{p}_0}{\bar{p}_\infty} - 1 \right] = 4I \left(\frac{\gamma+1}{2} \right)^{\frac{\gamma+1}{\gamma-1}} \gamma^{\frac{\gamma}{1-\gamma}}$$

or for $\gamma = 1.4$, $I = .453$

$$\frac{2}{\gamma M^2} \left[2I \frac{\bar{p}_0}{\bar{p}_\infty} - 1 \right] = 1.67$$

The results for $\theta_s = 10^\circ$ and 19° are shown as the triangles in figure 4 on the curve marked " $M = \infty$." For small values of θ_s , the results obtained by use of the Chart 6 of reference (5) are too inaccurate to have any meaning because it becomes impossible to read $\frac{\Delta \bar{p}}{\bar{p}}$ from the chart to enough

significant figures. Consequently, the empirical expression

$$\left(\frac{\Delta \bar{p}}{q}\right)_{c,s} = .01588 \left(\frac{\theta_s}{5}\right)^2, \quad (\theta_s \text{ in degrees}) \quad (33)$$

which fits the values of $\frac{\Delta \bar{p}}{q}$ obtained from reference (7) for $M = \infty$ with an error of less than one percent for $\theta_s \leq 10^\circ$, is used. From equation (33) and the assumption that $\frac{\Delta \bar{p}}{q}$ on a blunt cone is equal to that on a sharp cone with the same angle, it follows that

$$\left(\frac{\Delta \bar{p}}{q}\right)_c = \left(\frac{\Delta \bar{p}}{q}\right)_{c,s} \left(\frac{\theta}{\theta_s}\right)^2 \quad (34)$$

Moreover,

$$\frac{\theta}{\theta_s} = (1-H) \quad (35)$$

The portion of the curve for $M = \infty$ in figure 4 for $\theta_s < 10^\circ$ was calculated by use of equation (23) together with equations (34) and (35). In this calculation all powers of H greater than the second were neglected in the development of an expression for H_B . When equation (33) is used for $\left(\frac{\Delta \bar{p}}{q}\right)_{c,s}$, the result for $M = \infty$ and $\theta_s < 10^\circ$ is that

$$H_B = .7618 \times 10^{-4} \theta_s^2 \quad (\theta \text{ in degrees}) \quad (36)$$

The portion of the curve for $M = \infty$ for $\theta_s < 10^\circ$ in figure 4 was calculated by use of equation (34).

The indication from figure 4 is that H_B increases as the angle of the sharp-cone increases, and decreases as the Mach number increases. For a perfect gas, however, H_B does not decrease much below its values at $M = 4$.

Comparison with Experiment

Note that the present method estimates the change in pressure drag but not the change in friction or base drag caused by the change in nose shape. Consequently, exact agreement with experiment is not to be expected. With this remark in view, two sets of data are examined. The first set is contained in figure 16 of Section 16-14 of reference (1) in which is shown the dependence of the drag coefficient of a cone-cylinder on the cone angle at a Mach number of 2. The blunt cylinder is included. The present method, equation (11),

is used to predict the drag of the blunt cylinder from the given drag of the sharp nosed cone-cylinder. The results are shown in Table I. The maximum error is about 5 percent of the drag coefficient of the blunt cylinder. The same method can be used to predict the drag coefficient of a sharp nosed cone-cylinder from the known drag of a blunt cylinder. In this case, however, the percent error in the drag coefficient of the sharp cone-cylinder is much larger because the drag coefficient of a cone-cylinder is less than that of a blunt cylinder.

The second set of data is that of reference (2). In these experiments the nose of a cone of 24° 12' included angle was cut off at four distances from the tip. The value of ΔC_D calculated by the present method, that is, by equation (11), the value of C_D obtained by adding ΔC_D to C_D for the sharp cone, and the measured value of C_D are shown in Table II. Although the values of ΔC_D are inaccurate, the calculated values of C_D differ by no more than 16 percent from the measured values.

No experimental data seem to be available to test the predictions of the present method for the case in which a sharp cone is blunted without changing its nose length. Both the drag reduction caused by blunting a cone of fixed nose length and the value of H_B are obtained by using the calculated drag of a blunted cone. This drag is computed by using equation (11) to compute ΔC_D caused by blunting a sharp cone of the same angle as the blunt cone and then adding this value of ΔC_D to the value of C_D for the sharp cone. The equation used to compute ΔC_D , namely, equation (11), was also used to compute the values of ΔC_D listed in Table II. Because these values of ΔC_D are too large in all the cases listed, the present method overestimates the drag of blunt cones. Therefore, both the drag reduction caused by blunting a sharp cone of fixed nose length and the value of H_B would actually be larger than predicted. This inference is strengthened by the statement in reference (3) that at a Mach number of 6, the measured drag reduction caused by blunting a sharp cone by a hemisphere was greater than predicted. Both the method of reference (3) and the present method assume that the pressure on the side of the blunted cone is equal to that on a sharp cone of equal angle. Because the result of reference (3) is for a Mach number of 6, it appears that the inference that the present method overestimates ΔC_D is probably not limited to the Mach number range of the data in Table II. The cone angle of reference (3), namely, about 19° , is also somewhat different than for the data of Table II. The difference between theory and experiment is probably caused by the omission of skin friction and by the departure of the pressure from the sharp-cone pressure on the blunt cone behind the face-junction.

CONCLUDING REMARKS

A rapid method for estimation of the nose pressure drag coefficient in supersonic flow of a body formed by replacing all, or part, of its conical nose by a flat face is given.

The analysis agrees with the experimental observation that the drag coefficient of a flat-faced conical nose of fixed length decreases as the radius of the flat face increases from zero. Beyond a certain flat-face radius that depends on cone angle and Mach number, the drag rises above that of the sharp cone. The drag of a conical-nosed body, therefore, can be decreased and its volume increased by substituting a flat nose of the correct size.

The indication from the analysis is that the allowable blunting for no increase in drag over the sharp cone decreases slowly with increase in Mach number and more rapidly with decrease in sharp cone angle.

REFERENCES

- (1) Hoerner, Sighard F., "Fluid-Dynamic Drag," Published by author, 1958
- (2) Charters, A. C. and Stein, H., "The Drag of Projectiles with Truncated Cone Headshapes," Ballistic Research Laboratories Report No. 624, Mar 1952
- (3) Seiff, Alvin and Sandahl, Carl A., "The Effect of Nose Shape on the Drag of Bodies of Revolution at Zero Angle of Attack," NACA Conference on Aerodynamic Design Problems of Supersonic Guided Missiles, Ames Aero. Lab., Oct 2-3, 1951
- (4) Stoney, William E., Jr. and Markley, Thomas J., "Heat Transfer and Pressure Measurements on Flat-Faced Cylinders at a Mach Number of 2," NACA TN 4300, 1958
- (5) Ames Research Staff, "Equations, Tables, and Charts for Compressible Flow," NACA TR 1135, 1953
- (6) General Theory of High Speed Aerodynamics. W. R. Sears, ed., Vol. VI, High Speed Aerodynamics and Jet Propulsion, Princeton University Press, Princeton University, 1954
- (7) Kopal, Z., "Tables of Supersonic Flow Around Cones," Mass. Inst. of Tech. Report No. 1, 1947

Table I

PREDICTED DRAG COEFFICIENT OF BLUNT CYLINDER AND PERCENT ERROR
($M_{\infty}=2$)

Cone Angle	ΔC_D	Predicted C_D	Percent Error in C_D
11.3	1.34	1.62	5
14.1	1.29	1.66	2
18.4	1.19	1.64	4
26.6	.946	1.64	4
31.0	.787	1.62	5

Measured Drag Coefficient of Blunt Cylinder = 1.70.

Table II

PREDICTED ΔC_D AND C_D , MEASURED C_D , AND PERCENT ERROR IN C_D
FOR A CONE OF $24^\circ 12'$ INCLUDED ANGLE

$M = 1.65$

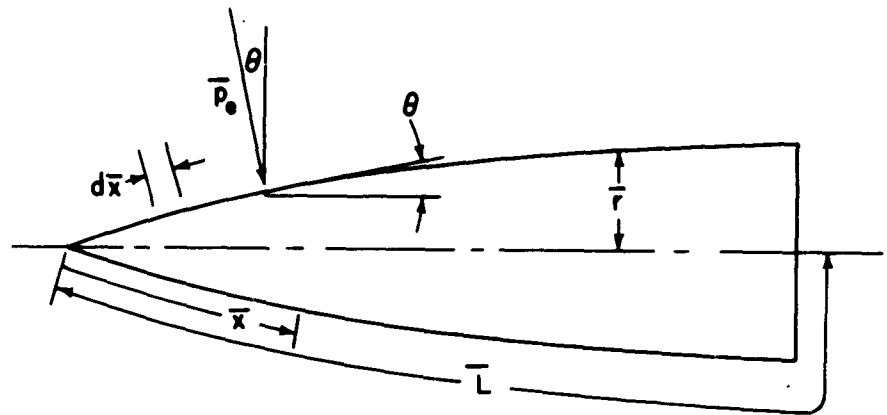
H	ΔC_D	C_D Calc.	C_D Meas.	Percent Error
0	<u> </u>	<u> </u>	.4061	<u> </u>
.165	.0334	.4395	.4233	4
.322	.1266	.5327	.4808	11
.483	.2862	.6923	.6000	16
.642	.5055	.9116	.7830	16

$M = 2.1$

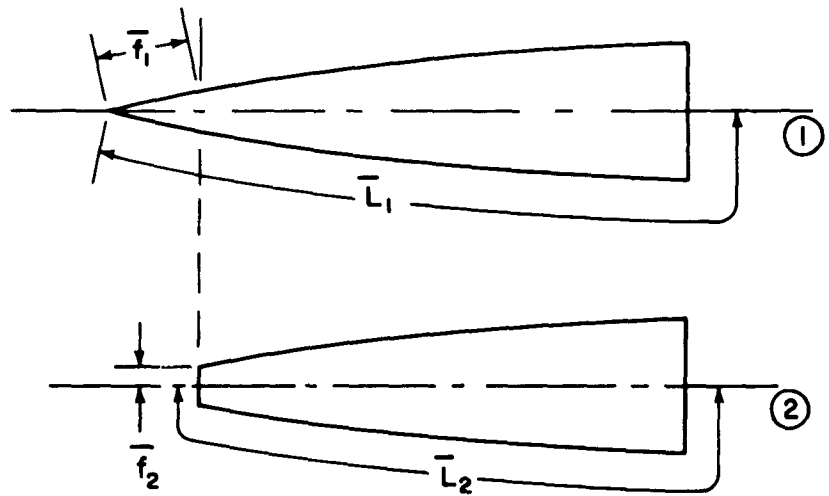
H	ΔC_D	C_D Calc.	C_D Meas.	Percent Error
0	<u> </u>	<u> </u>	.3478	<u> </u>
.165	.0367	.3845	.3652	5
.322	.1398	.4876	.4352	12
.483	.3146	.6624	.5962	11
.642	.5560	.9038	.8221	10

$M = 2.55$

H	ΔC_D	C_D Calc.	C_D Meas.	Percent Error
0	<u> </u>	<u> </u>	.3109	<u> </u>
.165	.0385	.3495	.3158	11
.322	.1468	.4577	.4140	11
.483	.3302	.6411	.5685	13
.642	.5830	.8939	.8200	9



(a)



(b)

FIG.1 COORDINATES AND BODY SHAPES

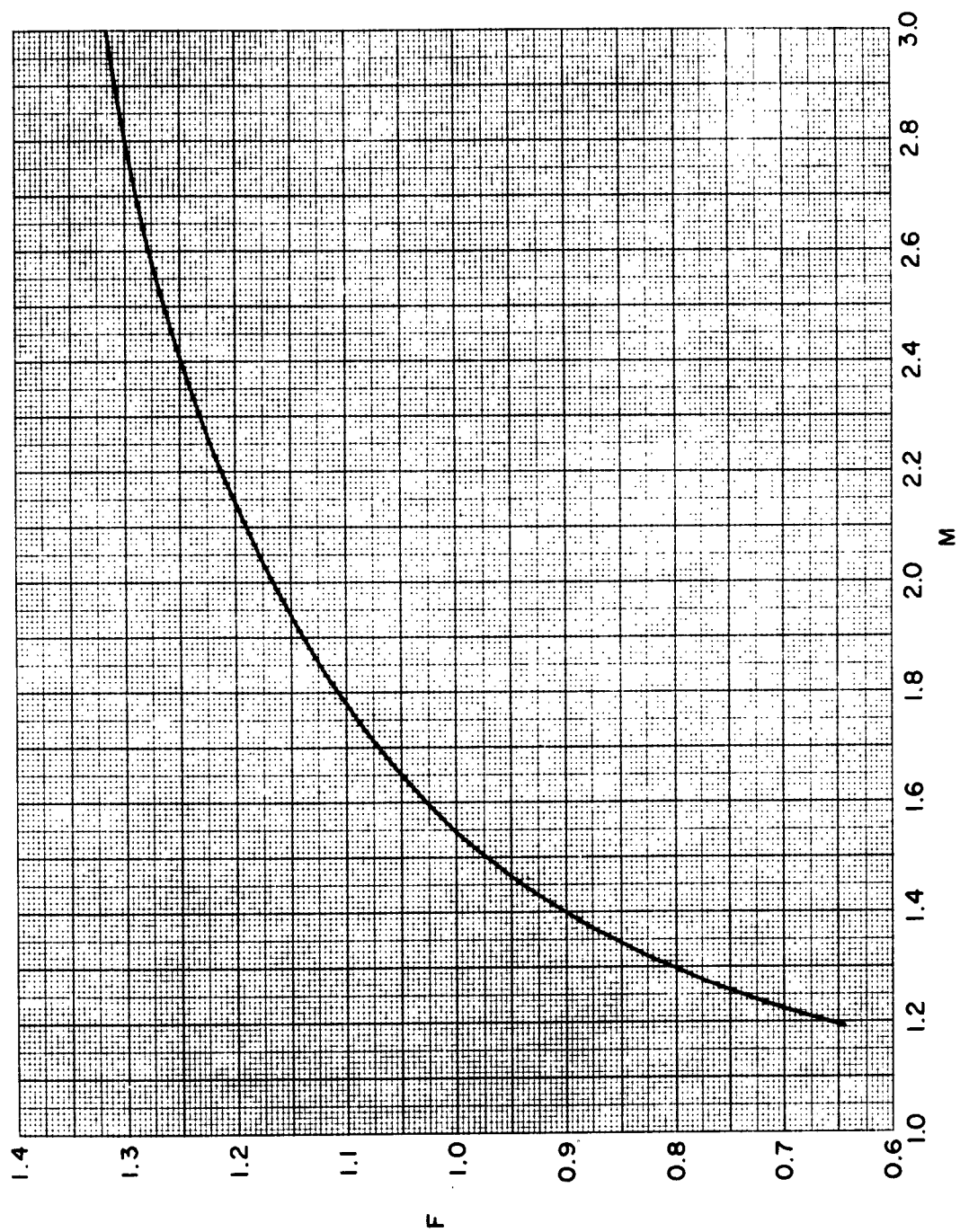


FIG. 2 DRAG FUNCTION F AS A FUNCTION OF MACH NUMBER FOR A 38° INCLUDED ANGLE CONE

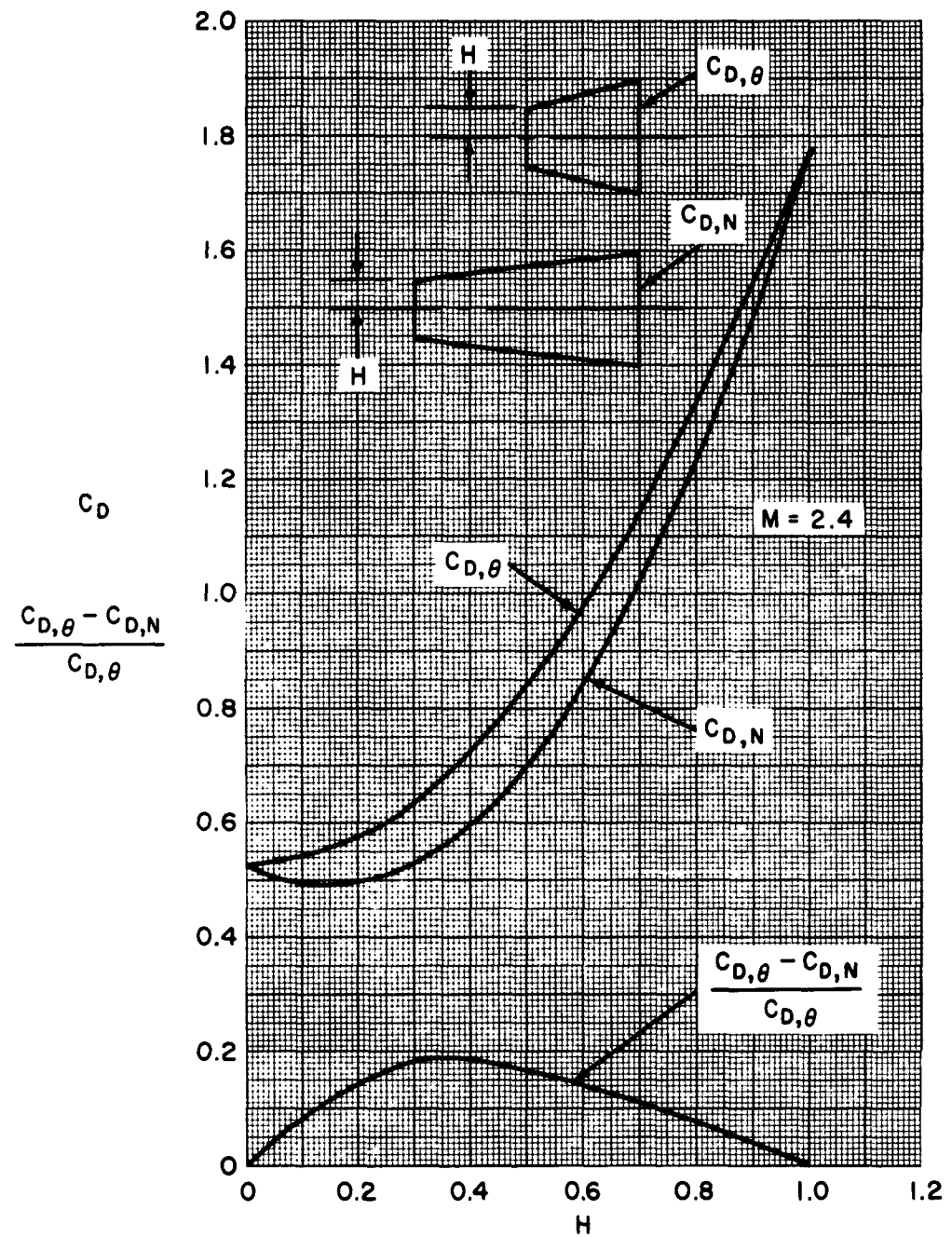


FIG. 3 NOSE DRAG COEFFICIENT AND INCREMENT IN NOSE DRAG COEFFICIENT FOR FLAT-FACE CONES OF CONSTANT ANGLE AND OF CONSTANT NOSE LENGTH

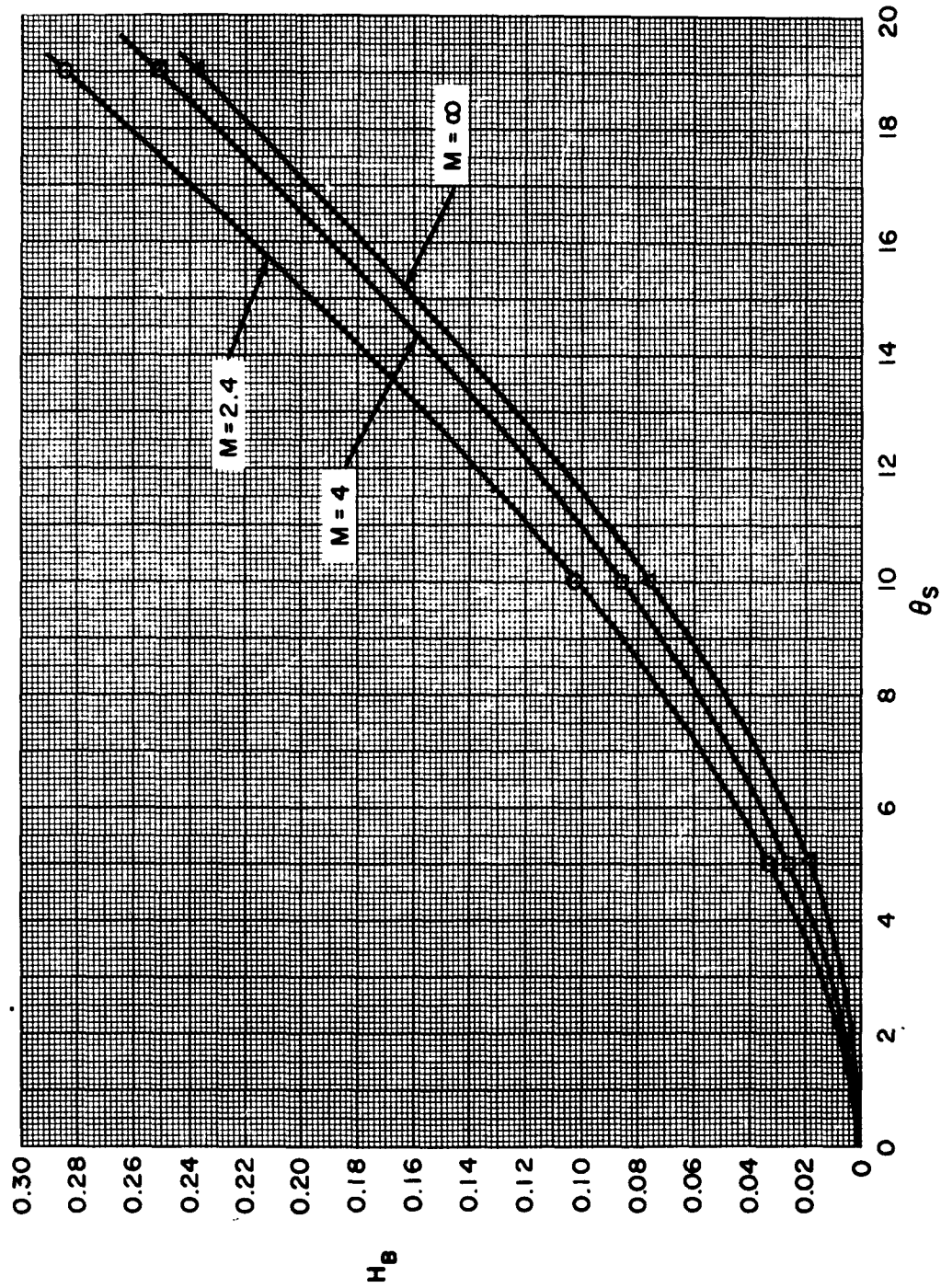


FIG. 4 VARIATION OF FLAT-FACE RADIUS H_B WITH ANGLE OF SHARP CONE θ_S FOR EQUAL DRAG OF FLAT-FACE CONE AND SHARP CONE

NOLTR 62-111

AERODYNAMICS DEPARTMENT
EXTERNAL DISTRIBUTION LIST (A1)

	<u>No. of Copies</u>
Chief, Bureau of Naval Weapons Department of the Navy Washington 25, D. C. Attn: DLI-30	1
Attn: R-14	1
Attn: RRRE-4	1
Attn: RMGA-413	1
Office of Naval Research Room 2709, T-3 Washington 25, D. C. Attn: Head, Mechanics Branch	1
Director, David Taylor Model Basin Aerodynamics Laboratory Washington 7, D. C. Attn: Library	1
Commander, U. S. Naval Ordnance Test Station China Lake, California Attn: Technical Library	1
Attn: Code 503	1
Attn: Code 406	1
Director, Naval Research Laboratory Washington 25, D. C. Attn: Code 2027	1
Commanding Officer Office of Naval Research Branch Office Box 39, Navy 100 Fleet Post Office New York, New York	1
NASA High Speed Flight Station Box 273 Edwards Air Force Base, California Attn: W. C. Williams	1
NASA Ames Research Center Moffett Field, California Attn: Librarian	1

NOLTR 62-111

AERODYNAMICS DEPARTMENT
EXTERNAL DISTRIBUTION LIST (A1)

	<u>No. of Copies</u>
NASA	
Langley Research Center	
Langley Field, Virginia	
Attn: Librarian	3
Attn: C. H. McLellan	1
Attn: J. J. Stack	1
Attn: Adolf Busemann	1
Attn: Comp. Res. Div.	1
Attn: Theoretical Aerodynamics Division	1
NASA	
Lewis Research Center	
21000 Brookpark Road	
Cleveland 11, Ohio	
Attn: Librarian	1
Attn: Chief, Propulsion Aerodynamics Div.	1
NASA	
1520 H Street, N. W.	
Washington 25, D. C.	
Attn: Chief, Division of Research Information	1
Attn: Dr. H. H. Kurzweg, Asst. Director of Research	1
Office of the Assistant Secretary of Defense (R&D)	
Room 3E1065, The Pentagon	
Washington 25, D. C.	
Attn: Technical Library	1
Research and Development Board	
Room 3D1041, The Pentagon	
Washington 25, D. C.	
Attn: Library	1
ASTIA	10
Arlington Hall Station	
Arlington 12, Virginia	
Commander, Pacific Missile Range	
Point Mugu, California	
Attn: Technical Library	1
Commanding General	
Aberdeen Proving Ground, Maryland	
Attn: Technical Information Branch	1
Attn: Ballistic Research Laboratory	1

**AERODYNAMICS DEPARTMENT
EXTERNAL DISTRIBUTION LIST (A1)**

	<u>No. of Copies</u>
Commander, Naval Weapons Laboratory Dahlgren, Virginia Attn: Library	1
Director, Special Projects Department of the Navy Washington 25, D. C. Attn: SP-2722	1
Director of Intelligence Headquarters, USAF Washington 25, D. C. Attn: AFOIN-3B	1
Headquarters - Aero. Systems Division Wright-Patterson Air Force Base Dayton, Ohio Attn: WWAD	2
Attn: RRLA-Library	1
Commander Air Force Ballistic Missile Division HQ Air Research & Development Command P. O. Box 262 Inglewood, California Attn: WDTLAR	1
Chief, Defense Atomic Support Agency Washington 25, D. C. Attn: Document Library	1
Headquarters, Arnold Engineering Development Center Air Research and Development Center Arnold Air Force Station, Tennessee Attn: Technical Library	1
Attn: AFOR	1
Attn: AEOIM	1
Commanding Officer, DOFL Washington 25, D. C. Attn: Library, Room 211, Bldg. 92	1
Commanding General Redstone Arsenal Huntsville, Alabama Attn: Mr. N. Shapiro (ORDDW-MRF)	1
Attn: Technical Library	1

NOLTR 62-111

**AERODYNAMICS DEPARTMENT
EXTERNAL DISTRIBUTION LIST (A1)**

	<u>No. of Copies</u>
NASA	
George C. Marshall Space Flight Center	
Huntsville, Alabama	
Attn: Dr. E. Geissler	1
Attn: Mr. T. Reed	1
Attn: Mr. H. Paul	1
Attn: Mr. W. Dahm	1
Attn: Mr. D. Burrows	1
Attn: Mr. J. Kingsbury	1
Attn: ORDAB-DA	1
APL/JHU (C/Now 7386)	
8621 Georgia Avenue	
Silver Spring, Maryland	
Attn: Technical Reports Group	2
Attn: Mr. D. Fox	1
Attn: Dr. F. Hill	1
Via: INSORD	
Air Force Systems Command	
Scientific & Technical Liaison Office	
Room 2305, Munitions Building	
Department of the Navy	
Washington 25, D. C.	
Attn: E. G. Haas	1

**AERODYNAMICS DEPARTMENT
EXTERNAL DISTRIBUTION LIST (A2)**

	<u>No. of Copies</u>
University of Minnesota Minneapolis 14, Minnesota	
Attn: Dr. E. R. G. Eckert	1
Attn: Heat Transfer Laboratory	1
Attn: Technical Library	1
Rensselaer Polytechnic Institute Troy, New York	
Attn: Dept. of Aeronautical Engineering	1
Dr. James P. Hartnett Department of Mechanical Engineering University of Delaware Newark, Delaware	1
Princeton University James Forrestal Research Center Gas Dynamics Laboratory Princeton, New Jersey	
Attn: Prof. S. Bogdonoff	1
Attn: Dept. of Aeronautical Engineering Library	1
Defense Research Laboratory The University of Texas P. O. Box 8029 Austin 12, Texas	
Attn: Assistant Director	1
Ohio State University Columbus 10, Ohio	
Attn: Security Officer	1
Attn: Aerodynamics Laboratory	1
Attn: Dr. J. Lee	1
Attn: Chairman, Dept. of Aero. Engineering	1
California Institute of Technology Pasadena, California	
Attn: Guggenheim Aero. Laboratory, Aeronautics Library	1
Attn: Jet Propulsion Laboratory	1
Attn: Dr. H. Liepmann	1
Attn: Dr. L. Lees	1
Attn: Dr. D. Coles	1
Attn: Mr. A. Roshko	1
Attn: Dr. J. Laufer	1
Case Institute of Technology Cleveland 6, Ohio	
Attn: G. Kuerti	1

AERODYNAMICS DEPARTMENT
EXTERNAL DISTRIBUTION LIST (A2)

	<u>No. of Copies</u>
North American Aviation, Inc. Aerophysics Laboratory Downing, California	
Attn: Dr. E. R. Van Driest	1
Attn: Missile Division (Library)	1
Department of Mechanical Engineering Yale University 400 Temple Street New Haven 10, Connecticut	
Attn: Dr. P. P. Wegener	1
Attn: Prof. N. A. Hall	1
MIT Lincoln Laboratory Lexington, Massachusetts	1
RAND Corporation 1700 Main Street Santa Monica, California	
Attn: Library, USAF Project RAND	1
Attn: Technical Communications	1
Mr. J. Lukasiewicz Chief, Gas Dynamics Facility ARO, Incorporated Tullahoma, Tennessee	1
Massachusetts Institute of Technology Cambridge 39, Massachusetts	
Attn: Prof. J. Kaye	1
Attn: Prof. M. Finston	1
Attn: Mr. J. Baron	1
Attn: Prof. A. H. Shapiro	1
Attn: Naval Supersonic Laboratory	1
Attn: Aero. Engineering Library	1
Polytechnic Institute of Brooklyn 527 Atlantic Avenue Freeport, New York	
Attn: Dr. A. Ferri	1
Attn: Dr. M. Bloom	1
Attn: Dr. P. Libby	1
Attn: Aerodynamics Laboratory	1
Brown University Division of Engineering Providence, Rhode Island	
Attn: Prof. R. Probstein	1
Attn: Prof. C. Lin	1
Attn: Librarian	1

NOLTR 62-111

**AERODYNAMICS DEPARTMENT
EXTERNAL DISTRIBUTION LIST (A2)**

	<u>No. of Copies</u>
Air Ballistics Laboratory Army Ballistic Missile Agency Huntsville, Alabama	1
Applied Mechanics Reviews Southwest Research Institute 8500 Culebra Road San Antonio 6, Texas	1
BuWeps Representative Aerojet-General Corporation 6352 N. Irwindale Avenue Azusa, California	1
Boeing Airplane Company Seattle, Washington Attn: J. H. Russell Attn: Research Library	1 1
United Aircraft Corporation 400 Main Street East Hartford 8, Connecticut Attn: Chief Librarian Attn: Mr. W. Kuhrt, Research Dept. Attn: Mr. J. G. Lee	1 2 1
Hughes Aircraft Company Florence Avenue at Teale Streets Culver City, California Attn: Mr. D. J. Johnson R&D Technical Library	1
McDonnell Aircraft Corporation P. O. Box 516 St. Louis 3, Missouri	1
Lockheed Missiles and Space Company P. O. Box 504 Sunnyvale, California Attn: Dr. L. H. Wilson Attn: Mr. M. Tucker Attn: Mr. R. Smelt	1 1 1
The Martin Company Baltimore 3, Maryland Attn: Library Attn: Chief Aerodynamicist	1 1

NOLTR 62-111

AERODYNAMICS DEPARTMENT
EXTERNAL DISTRIBUTION LIST (A2)

	<u>No. of Copies</u>
CONVAIR	
A Division of General Dynamics Corporation Fort Worth, Texas	
Attn: Library	1
Attn: Theoretical Aerodynamics Group	1
Purdue University	
School of Aeronautical & Engineering Sciences LaFayette, Indiana	
Attn: R. L. Taggart, Library	1
University of Maryland	
College Park, Maryland	
Attn: Director	2
Attn: Dr. J. Burgers	1
Attn: Librarian, Engr. & Physical Sciences	1
Attn: Librarian, Institute for Fluid Dynamics and Applied Mathematics	1
University of Michigan	
Ann Arbor, Michigan	
Attn: Dr. A. Kuethe	1
Attn: Dr. O. Laporte	1
Attn: Department of Aeronautical Engineering	1
Stanford University	
Palo Alto, California	
Attn: Applied Mathematics & Statistics Lab.	1
Attn: Prof. D. Bershader, Dept. of Aero. Engr.	1
Cornell University	
Graduate School of Aeronautical Engineering Ithaca, New York	
Attn: Prof. W. R. Sears	1
The Johns Hopkins University	
Charles and 34th Streets Baltimore, Maryland	
Attn: Dr. F. H. Clauser	1
Attn: Dr. M. Morkovin	1
University of California	
Berkeley 4, California	
Attn: G. Maslach	1
Attn: Dr. S. Schaaf	1
Attn: Dr. Holt	1
Attn: Institute of Engineering Research	1

NOLTR 62-111
AERODYNAMICS DEPARTMENT
EXTERNAL DISTRIBUTION LIST (A2)

	<u>No. of Copies</u>
Cornell Aeronautical Laboratory, Inc.	
4455 Genesee Street	
Buffalo 21, New York	
Attn: Librarian	1
Attn: Dr. Franklin Moore	1
Attn: Dr. J. G. Hall	1
 University of Minnesota	
Rosemount Research Laboratories	
Rosemount, Minnesota	
Attn: Technical Library	1
 Director, Air University Library	1
Maxwell Air Force Base, Alabama	
 Douglas Aircraft Company, Inc.	
Santa Monica Division	
3000 Ocean Park Boulevard	
Santa Monica California	
Attn: Chief Missiles Engineer	1
Attn: Aerodynamics Section	1
 General Motors Corporation	
Defense Systems Division	
Santa Barbara, California	
Attn: Dr. A. C. Charters	1
 CONVAIR	1
A Division of General Dynamics Corporation	
Daingerfield, Texas	
 CONVAIR	
Scientific Research Laboratory	
5001 Kearney Villa Road	
San Diego 11, California	
Attn: Mr. M. Sibulkin	1
Attn: Asst. to the Director of	
Scientific Research	1
Attn: Dr. B. M. Leadon	1
Attn: Library	1
 Republic Aviation Corporation	
Farmingdale, New York	
Attn: Technical Library	1
 General Applied Science Laboratories, Inc.	
Merrick and Stewart Avenues	
Westbury, L. I., New York	
Attn: Mr. Walter Daskin	1
Attn: Mr. R. W. Byrne	1

NOLTR 62-111

AERODYNAMICS DEPARTMENT
EXTERNAL DISTRIBUTION LIST (A2)

	<u>No. of Copies</u>
Arnold Research Organization, Inc. Tullahoma, Tennessee	
Attn: Technical Library	1
Attn: Chief, Propulsion Wind Tunnel	1
Attn: Dr. J. L. Potter	1
General Electric Company Missile and Space Vehicle Department 3198 Chestnut Street Philadelphia, Pennsylvania	
Attn: Larry Chasen, Mgr. Library	2
Attn: Mr. R. Kirby	1
Attn: Dr. J. Farber	1
Attn: Dr. G. Sutton	1
Attn: Dr. J. D. Stewart	1
Attn: Dr. S. M. Scala	1
Attn: Dr. H. Lew	1
Attn: Mr. J. Persh	1
Eastman Kodak Company Navy Ordnance Division 50 West Main Street Rochester 14, New York	
Attn: W. B. Forman	2
Library	3
AVCO-Everett Research Laboratory 2385 Revere Beach Parkway Everett 49, Massachusetts	
AVCO-Everett Research Laboratory 201 Lowell Street Wilmington, Massachusetts	
Attn: Mr. F. R. Riddell	1
AER, Incorporated 158 North Hill Avenue Pasadena, California	1
Armour Research Foundation 10 West 35th Street Chicago 16, Illinois	
Attn: Dept. M	2
Attn: Dr. Paul T. Torda	1
Chance-Vought Aircraft, Inc. Dallas, Texas	
Attn: Librarian	2

NOLTR 62-111

AERODYNAMICS DEPARTMENT
EXTERNAL DISTRIBUTION LIST (A2)

	<u>No. of Copies</u>
National Science Foundation 1951 Constitution Avenue, N. W. Washington 25, D. C. Attn: Engineering Sciences Division	1
New York University University Heights New York 53, New York Attn: Department of Aeronautical Engineering	1
New York University 25 Waverly Place New York 3, New York Attn: Library, Institute of Math. Sciences	1
NORAIR A Division of Northrop Corp. Hawthorne, California Attn: Library	1
Northrop Aircraft, Inc. Hawthorne, California Attn: Library	1
Gas Dynamics Laboratory Technological Institute Northwestern University Evanston, Illinois Attn: Library	1
Pennsylvania State University University Park, Pennsylvania Attn: Library, Dept. of Aero. Engineering	1
The Ramo-Wooldridge Corporation 8820 Bellanca Avenue Los Angeles 45, California	1
Gifts and Exchanges Fondren Library Rice Institute P. O. Box 1892 Houston 1, Texas	1
University of Southern California Engineering Center Los Angeles 7, California Attn: Librarian	1

NOLTR 62-111

AERODYNAMICS DEPARTMENT
EXTERNAL DISTRIBUTION LIST (A2)

	<u>No. of Copies</u>
Commander Air Force Flight Test Center Edwards Air Force Base Muroc, California Attn: FTOTL	1
Air Force Office of Scientific Research Holloman Air Force Base Alamogordo, New Mexico Attn: SRLTL	1
The Editor Battelle Technical Review Battelle Memorial Institute 505 King Avenue Columbus 1, Ohio	1
Douglas Aircraft Company, Inc. El Segundo Division El Segundo, California	1
Fluidyne Engineering Corp. 5740 Wayzata Blvd. Golden Valley Minneapolis 16, Minnesota	1
Grumman Aircraft Engineering Corp. Bethpage, L. I., New York	1
Lockheed Missile and Space Company P. O. Box 551 Burbank, California Attn: Library	1
Marquardt Aircraft Corporation 7801 Havenhurst Van Nuys, California	1
The Martin Company Denver, Colorado Attn: Library	1
Mississippi State College Engineering and Industrial Research Station Aerophysics Department P. O. Box 248 State College, Mississippi	1

NOLTR 62-111

**AERODYNAMICS DEPARTMENT
EXTERNAL DISTRIBUTION LIST (A2)**

	<u>No. of Copies</u>
Lockheed Missile and Space Company 3251 Hanover Street Palo Alto, California Attn: Mr. J. A. Laurmann Attn: Library	1
General Electric Company Research Laboratory Schenectady, New York Attn: Dr. H. T. Nagamatsu Attn: Library	1
Fluid Dynamics Laboratory Mechanical Engineering Department Stevens Institute of Technology Hoboken, New Jersey Attn: Dr. R. H. Page, Director	1
Department of Mechanical Engineering University of Arizona Tucson, Arizona Attn: Dr. E. K. Parks	1
Vitro Laboratories 200 Pleasant Valley Way West Orange, New Jersey Attn: Dr. Charles Sheer	1
Department of Aeronautical Engineering University of Washington Seattle 5, Washington Attn: Prof. R. E. Street Attn: Library	1 1
Aeronautical Engineering Review 2 East 64th Street New York 21, New York	1
Institute of the Aerospace Sciences 2 East 64th Street New York 21, New York Attn: Managing Editor Attn: Library	1 1
Department of Aeronautics United States Air Force Academy Colorado	1

NOLTR 62-111

**AERODYNAMICS DEPARTMENT
EXTERNAL DISTRIBUTION LIST (A2)**

	<u>No. of Copies</u>
MHD Research, Inc. Newport Beach, California Attn: Dr. V. H. Blackman, Technical Director	1
University of Alabama College of Engineering University, Alabama Attn: Prof. C. H. Bryan, Head Dept. of Aeronautical Engineering	1
Office of Naval Research Bldg. T-3, Department of the Navy 17th and Constitution Avenue Washington 25, D. C. Attn: Mr. Ralph D. Cooper, Head Fluid Dynamics Branch	1
ARDE Associates 100 W. Century Road Paramus, New Jersey Attn: Mr. Edward Cooperman	1
Aeronautical Research Associates of Princeton 50 Washington Road Princeton, New Jersey Attn: Dr. C. duP. Donaldson, President	1
Daniel Guggenheim School of Aeronautics Georgia Institute of Technology Atlanta, Georgia Attn: Prof. A. L. Ducoffe	1
University of Cincinnati Cincinnati, Ohio Attn: Prof. R. P. Harrington, Head Dept. of Aeronautical Engineering	1
Virginia Polytechnic Institute Dept. of Aerospace Engineering Blacksburg, Virginia Attn: Mr. R. T. Keefe Attn: Library	1 1
IBM Federal System Division 7220 Wisconsin Avenue Bethesda, Maryland Attn: Dr. I. Korobkin	1

NOLTR 62-111

**AERODYNAMICS DEPARTMENT
EXTERNAL DISTRIBUTION LIST (A2)**

	<u>No. of Copies</u>
Superintendent U. S. Naval Postgraduate School Monterey, California Attn: Technical Reports Section Library	1
National Bureau of Standards Washington 25, D. C. Attn: Chief, Fluid Mechanics Section	1
North Carolina State College Raleigh, North Carolina Attn: Prof. R. W. Truitt, Head Dept. of Mechanical Engineering	1
Attn: Division of Engineering Research Technical Library	1
Prof. A. Robinson Department of Mathematics University of California Los Angeles, California	1

CATALOGING INFORMATION FOR LIBRARY USE

BIBLIOGRAPHIC INFORMATION

	DESCRIPTORS	CODES	DESCRIPTORS	CODES
SOURCE	NOL. technical report	NOLTR	Unclassified - 15	U015
REPORT NUMBER	62-111	62-111		
REPORT DATE	1 December 1962	1262		

SUBJECT ANALYSIS OF REPORT

	DESCRIPTORS	CODES	DESCRIPTORS	CODES
Drag	DRAG		Reentry	REEN
Bodies	BODY		Mathematics	MATH
Truncated	TRCT		Equations	EQUA
Nose	NOSE			
Conical	CONE			
Supersonic	SUPR			
Flow	FLOW			
Pressure	PRES			
Flat	FLAT			
Approximate	APPR			
Analysis	ANAL			
Aerodynamics	AERD			

Naval Ordnance Laboratory, White Oak, Md.

(NOL technical report 62-111)

APPROXIMATE ANALYSIS OF EFFECT ON DRAG OF TRUNCATING THE CONICAL NOSE OF A BODY OF REVOLUTION IN SUPERSONIC FLOW (U), by Neal Tetervin. 1 Dec. 1962. 15p tables. (Aerodynamics research report 183) Task NOL-363. UNCLASSIFIED

A rapid method for estimating the nose pressure drag coefficient in supersonic flow of a body formed by replacing all, or part of, its conical nose by a flat face is derived. The analysis, although rough, agrees with the experimental observation that the drag coefficient of a flat-faced cone of fixed length decreases as the radius of the flat face increases from zero. After reaching a minimum, the drag coefficient rises above that of the sharp-tipped cone.

1. Bodies -
- Aerodynamics
2. Bodies -
- Bodies -
- Oscillations
3. Noses -
- Drag
- I. Title
- II. Tetervin,
- III. Neal
- IV. Series
- Project

Abstract card is unclassified.

Naval Ordnance Laboratory, White Oak, Md.

(NOL technical report 62-111)

APPROXIMATE ANALYSIS OF EFFECT ON DRAG OF TRUNCATING THE CONICAL NOSE OF A BODY OF REVOLUTION IN SUPERSONIC FLOW (U), by Neal Tetervin. 1 Dec. 1962. 15p tables. (Aerodynamics research report 183) Task NOL-363. UNCLASSIFIED

A rapid method for estimating the nose pressure drag coefficient in supersonic flow of a body formed by replacing all, or part of, its conical nose by a flat face is derived. The analysis, although rough, agrees with the experimental observation that the drag coefficient of a flat-faced cone of fixed length decreases as the radius of the flat face increases from zero. After reaching a minimum, the drag coefficient rises above that of the sharp-tipped cone.

1. Bodies -
- Aerodynamics
2. Bodies -
- Bodies -
- Oscillations
3. Noses -
- Drag
- I. Title
- II. Tetervin,
- III. Neal
- IV. Series
- Project

Abstract card is unclassified.

Naval Ordnance Laboratory, White Oak, Md.

(NOL technical report 62-111)

APPROXIMATE ANALYSIS OF EFFECT ON DRAG OF TRUNCATING THE CONICAL NOSE OF A BODY OF REVOLUTION IN SUPERSONIC FLOW (U), by Neal Tetervin. 1 Dec. 1962. 15p tables. (Aerodynamics research report 183) Task NOL-363. UNCLASSIFIED

A rapid method for estimating the nose pressure drag coefficient in supersonic flow of a body formed by replacing all, or part of, its conical nose by a flat face is derived. The analysis, although rough, agrees with the experimental observation that the drag coefficient of a flat-faced cone of fixed length decreases as the radius of the flat face increases from zero. After reaching a minimum, the drag coefficient rises above that of the sharp-tipped cone.

1. Bodies -
- Aerodynamics
2. Bodies -
- Bodies -
- Oscillations
3. Noses -
- Drag
- I. Title
- II. Tetervin,
- III. Neal
- IV. Series
- Project

Abstract card is unclassified.

Naval Ordnance Laboratory, White Oak, Md.

(NOL technical report 62-111)

APPROXIMATE ANALYSIS OF EFFECT ON DRAG OF TRUNCATING THE CONICAL NOSE OF A BODY OF REVOLUTION IN SUPERSONIC FLOW (U), by Neal Tetervin. 1 Dec. 1962. 15p tables. (Aerodynamics research report 183) Task NOL-363. UNCLASSIFIED

A rapid method for estimating the nose pressure drag coefficient in supersonic flow of a body formed by replacing all, or part of, its conical nose by a flat face is derived. The analysis, although rough, agrees with the experimental observation that the drag coefficient of a flat-faced cone of fixed length decreases as the radius of the flat face increases from zero. After reaching a minimum, the drag coefficient rises above that of the sharp-tipped cone.

1. Bodies -
- Aerodynamics
2. Bodies -
- Bodies -
- Oscillations
3. Noses -
- Drag
- I. Title
- II. Tetervin,
- III. Neal
- IV. Series
- Project

Abstract card is unclassified.